OPEN ACCESS Freely available online

PLoS GENETICS

The FUN30 Chromatin Remodeler, Fft3, Protects Centromeric and Subtelomeric Domains from Euchromatin Formation

Annelie Strålfors[1], Julian Walfridsson[1,2], Hasanuzzaman Bhuiyan[2], Karl Ekwall[1,2]*

1 Department of Biosciences and Medical Nutrition, Center for Biosciences, Karolinska Institutet, Huddinge, Sweden, **2** University College Södertörn, Department of Life Sciences, Huddinge, Sweden

Abstract

The chromosomes of eukaryotes are organized into structurally and functionally discrete domains. This implies the presence of insulator elements that separate adjacent domains, allowing them to maintain different chromatin structures. We show that the Fun30 chromatin remodeler, Fft3, is essential for maintaining a proper chromatin structure at centromeres and subtelomeres. Fft3 is localized to insulator elements and inhibits euchromatin assembly in silent chromatin domains. In its absence, euchromatic histone modifications and histone variants invade centromeres and subtelomeres, causing a mis-regulation of gene expression and severe chromosome segregation defects. Our data strongly suggest that Fft3 controls the identity of chromatin domains by protecting these regions from euchromatin assembly.

Citation: Strålfors A, Walfridsson J, Bhuiyan H, Ekwall K (2011) The FUN30 Chromatin Remodeler, Fft3, Protects Centromeric and Subtelomeric Domains from Euchromatin Formation. PLoS Genet 7(3): e1001334. doi:10.1371/journal.pgen.1001334

Editor: Hiten D. Madhani, University of California San Francisco, United States of America

Received July 26, 2010; **Accepted** February 11, 2011; **Published** March 17, 2011

Funding: This work was supported by the Swedish Cancer Found, the Swedish Research Council (VR), and the Göran Gustafsson foundation for research in Natural Sciences and Medicine. The funders had no role in study design, data collection and analysis, decision to publish, or preparation of the manuscript.

Competing Interests: The authors have declared that no competing interests exist.

* E-mail: karl.ekwall@ki.se

Introduction

The eukaryotic genome is organized into chromosomal domains of distinct structure and function. One type of chromatin structure, termed euchromatin, is decondensed and accessible most of the time and condenses only during mitosis. In contrast, the compacted heterochromatin remains condensed throughout the cell cycle except during S phase. In general, euchromatin contains transcriptionally active genes, whereas heterochromatin contains repetitive sequences and relatively few silenced genes.

Post-translational histone modifications have a crucial role in organizing chromosomes into different domains. Euchromatin is enriched in methylation of histone H3 at lysine 4 (H3K4me) and contains hyperacetylated histones [1–4]. This generates an open chromatin fiber, enabling better access of the transcription machinery. In contrast, heterochromatin lacks H3K4me, but is methylated at lysine 9 of histone H3 (H3K9me) and has low levels of histone acetylation [1,5]. H3K9me recruits HP1 chromo-domain proteins which packages the chromatin into an inaccessible configuration that silences genes transcriptionally [6].

Active and silent chromatin domains are often juxtaposed along the chromosomes and this organization demands a mechanism to separate them. The borders between these functionally antagonistic chromatin domains are often defined by specialized DNA sequences, known as insulators. Insulators are generally divided into two subclasses; enhancer-blocking insulators that prevent an enhancer from communicating with a promoter when positioned between the two, and barrier insulators that limit the spread of heterochromatin into the adjacent domain [7]. How certain DNA sequences can insulate chromatin domains is uncertain. It has been suggested that the insulators recruits chromatin-modifying factors, which would counteract the propagation of adjacent chromatin structures [8,9]. Alternatively, another model suggests that the insulators could form loops and tether chromatin to fixed nuclear substrates, resulting in the formation of topologically distinct active and inactive domains [10,11].

The fission yeast, *Schizosaccharomyces pombe*, is an excellent model system to study chromatin domains. Its three chromosomes are structurally similar to those of more complex eukaryotes, and many factors involved in heterochromatin assembly are conserved [12]. *S. pombe* chromosomes contain relatively large blocks of heterochromatin at centromeres, subtelomeres, tandem rDNA arrays and at the silent mating-type region [1].

Three structurally and genomically distinct types of insulators have been described in *S. pombe*. The most studied boundary is the cluster of tRNA genes located between centromeric chromatin and the flanking pericentric heterochromatin domains. Removal of these genes causes spreading of heterochromatin and silencing of reporter genes [13]. The insulator function seems to be a general property of tRNA genes, since replacement of centromeric tRNAs with noncentromeric tRNA isotypes does not affect the function of the centromeric boundary [14]. The mechanisms of tRNA boundary function is not completely understood, but it has been shown that the transcription factor TFIIIC and RNA polymerase III are required [14]. The Pol III initiation complex is thought to exclude histones from the barrier element, thereby generating a nucleosome-free region that restricts the spreading of silent chromatin [15]. Moreover, two histone demethylases, Lsd1 and Lsd2, associate with centromeric tRNA genes, and the deletion of Lsd1 results in the propagation of pericentric heterochromatin beyond the tRNA boundaries [16].

Author Summary

Active and inactive chromatin domains are often juxtaposed along the chromosome arms, and this demands mechanisms that separate them apart. This is performed by insulators that block the spreading of chromatin domains beyond their natural borders. Here, we show that an ATP-dependent chromatin remodeler, Fission yeast fun thirty (Fft3), is localized at known insulator elements and protects centromeric and subtelomeric chromatin domains. When Fft3 is absent, euchromatin invades the centromere and subtelomeres, causing a change in histone modification, incorrect incorporation of histone variants, mis-regulation of gene expression, and severe chromosome segregation defects. We conclude that Fft3 controls the identity of these chromatin domains by shielding them from euchromatin.

A second type of insulator is present outside the centromeric heterochromatin domains. Two inverted repeats, *IRC*, flank the left and right border of centromeres 1 and 3 [1,11]. The mode of action of the centromeric *IRC* barrier is unknown. However, it has been shown that it is independent of TFIIIC and Pol III [11].

Another type of inverted repeats, *IR* elements, flank the silent mating type cassettes [2,17]. They contain several Pol III B Box motifs and their boundary activity requires the association of TFIIIC, but not Pol III [11].

In this study, we have identified a SNF2 family ATP-dependent chromatin-remodeling factor, *F*ission yeast *f*un *t*hirty (Fft3), required for proper chromatin structure at centromeres and subtelomeres. Fft3 is localized to known insulator elements and in its absence, euchromatin invades centromeres and subtelomeres, causing a change in histone modifications, histone variant localization, mis-regulation of gene expression and chromosome segregation defects. Based on this phenotype of *fft3Δ*, we suggest that Fft3 controls the identity of these chromatin domains by protecting them from euchromatin formation.

Results

Fft3 is required for the assembly of functional centromeric chromatin

The Fun30 chromatin remodeler was identified in a screen for genes that affect chromosome stability in budding yeast [18]. This finding prompted us to investigate whether the *S. pombe* Fun30 homolog, Fft3, also has a role in chromosome stability.

To test this we constructed wild type and *fft3Δ* mutant strains bearing the Ch16 mini-chromosome. When this mini-chromosome is lost the cells form red rather than white colonies on limited adenine plates. By scoring the frequency of half-sectored colonies, the rate of chromosome loss per division can be calculated. The *fft3Δ* mutant shows a very high frequency of mini-chromosome loss (11%, Figure 1A) compared to wild type (0.13%). This result was confirmed by DAPI staining of mitotic chromosomes. As expected, *fft3Δ* cells show a higher rate of unequal chromosome segregation compared to wild type. Five percent of *fft3Δ* cells show a segregation defect in which none of the chromosomes separate. Instead, all DAPI-stained material stays on one side of the septum (Figure 1B). This phenotype is typical for proteins important for kinetochore formation [19,20].

The *S. pombe* centromeres consist of a central core domain (*cnt*), where the kinetochore is formed, surrounded by inverted repeats. Closest to the *cnt* are the inner repeats (*imr*) flanked by the outer repeats (*otr*), which are composed of *dg* and *dh* elements [21,22] (Figure S1). The *otr* regions are assembled into heterochromatin [23,24]. The central core domain possesses a different chromatin structure from the outer repeats. It is not heterochromatic, though there is transcriptional silencing. Placement of a *ura4+* gene within this centromeric region results in its transcriptional silencing [25]. We found that cells carrying a deletion for *fft3* show an increased

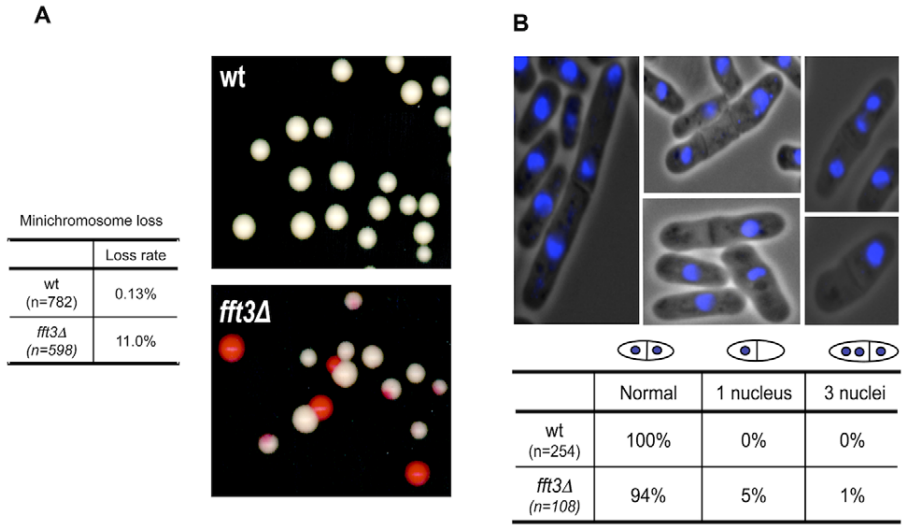

Figure 1. The Fun30 ATP-dependent chromatin remodeler Fft3 is required for accurate chromosome segregation. A) Left: A table showing data from the Ch16 mini-chromosome loss colony color-sectoring assay. Wild type (Hu199) and *fft3Δ* (Hu1666) colonies containing a mini-chromosome were picked from plates selecting for the mini-chromosome (Ade-), and plated onto YE+ low adenine plates. The colonies retaining the mini-chromosome are white, and loss events result in red sectors. The mini-chromosome loss frequency was quantified by determining the amount of half-sectored colonies. Right: A photograph showing the red-sectoring phenotype of *fft3Δ* cells. B) Top: Microscope images showing *fft3Δ* (Hu1867) cells stained with DAPI. Bottom: A table showing the frequencies of aberrant mitosis in wt (Hu29) and *fft3Δ* (Hu1867) cells.
doi:10.1371/journal.pgen.1001334.g001

sensitivity to FOA as compared to wt cells when the *ura4+* gene is inserted to the central core domain (Figure S1A), indicating that the *ura4+* genes is upregulated. A slight upregulation of the *ura4+* genes was also supported by RT-PCR analysis (Figure S1B).

Taken together our findings suggest that Fft3 contributes to the unique chromatin structure underlying the kinetochore.

Fft3 is localized at tRNA and IRC insulator elements

To investigate whether Fft3 has a direct role at centromeres, we analyzed the localization of Fft3-myc fusion protein using a genome-wide ChIP-chip assay. The experiment clearly revealed that Fft3 is located at the central core domains of all three centromeres (Figure 2 and Figure S2). In this domain histone H3 is replaced by the variant histone Cnp1 (*S. pombe* homolog of CENP-A). The Cnp1 chromatin is surrounded by heterochromatin methylated at lysine 9 of histone H3 [1,23]. At the transition between the central core and the *otr* regions we observed a sharp decrease in Fft3 localization. Fft3 continues to be depleted from the entire heterochromatin domains in both directions until the border between *otr* and the surrounding euchromatin, where we also detected prominent peaks of Fft3. A similar localization pattern was observed for chromosomes 1 and 2 (Figure S2).

Clusters of tRNA genes demark the transition between the *imr/cnt* and *otr* at all centromeres in *S. pombe*. These genes have been shown to act as insulators and prevent heterochromatin from spreading into the Cnp1-containing chromatin [13]. Notably, our ChIP-chip data shows that Fft3 is enriched over these tRNA genes. tRNA clusters are also present at five of the six centromere extremities. Fft3 is enriched over these tRNA clusters as well. Fft3 localization is not restricted to centromeric tRNA genes. We also found that Fft3 was enriched (2-fold) over 156 out of the 175 (89%) tRNA genes throughout the genome (data not shown).

An additional centromeric insulator element has been identified in *S. pombe*. At centromeres 1 and 3 the boundaries between pericentromeric heterochromatin and surrounding euchromatin coincide with the location of *IRC* elements [1]. Deletion of *IRC1-L* causes spreading of H3K9me from the centromere into the surrounding euchromatin, suggesting that these elements function as heterochromatin barriers [2]. Our Fft3 occupancy map clearly shows that Fft3 is also enriched over these elements (Figure 2 and Figure S2).

Taken together, our Chip-chip analysis demonstrates Fft3 occupancy over all known centromeric insulator elements in *S. pombe*, suggesting that the remodeling factor could have a function at these boundaries.

The chromatin structure of centromeric domains and boundaries is altered in *fft3Δ* cells

Most tRNA genes reside in nucleosome free regions and it has been suggested that this nucleosome-free gap is sufficient to provide a boundary function for the tRNA genes [26]. In budding yeast, the RNA Pol III complex and a chromatin remodeler, RSC, are thought to be involved in generating such a histone-depleted region [9]. To test whether the Fun30 remodeler could have a function in disassembling nucleosomes over centromeric tRNA genes we analyzed the distribution of histone H3 by ChIP-chip experiments.

Our data shows that H3 is enriched over the entire pericentromeric heterochromatin regions (Figure 3A (blue), and Figure S3). As expected, we observed a sharp decrease in H3 density over the tRNA genes surrounding the central domain, and at the tRNA and *IRC* elements flanking the right and left borders of the pericentric region. The H3 levels are low over the central domain, where instead the histone H3 variant, Cnp1 is enriched (Figure 3C (red)). ChIP-chip analysis of *fft3Δ* mutant cells revealed that H3 remained depleted over the tRNA genes and IRC boundary element, indicating that Fft3 is not involved in evicting histones from the insulators. However, our analysis showed that in *fft3Δ* cells, H3 appears in the *imr* regions (Figure 3A; blue). This increase of H3 was validated by quantitative PCR of ChIP samples (Figure 3D). We found a 3.5 fold increase of H3 levels at *imr3* in *fft3Δ* vs wt (P value 0.0002; T-test). Consistent with this, the Cnp1 levels were 2.7 fold reduced (P value 0.001; T-test) at *imr3* in *fft3Δ*

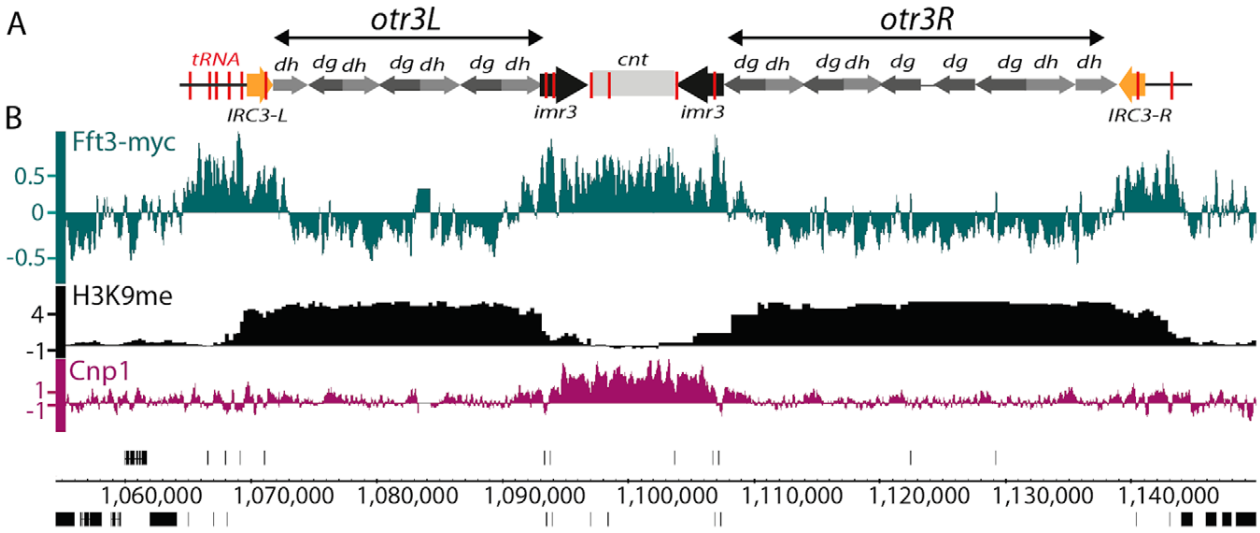

Figure 2. Fft3 associates with known centromeric insulators and the central core domain. A) A schematic presentation of centromere 3. tRNA genes are marked in red and the *IRC* elements in yellow. B) A genome browser view of *cen3* showing the ChIP-chip occupancy profile for Fft3-myc (green), H3K9me2 (black) and Cnp1 (purple). Data on the Y-axis are presented in log2 scale and the X-axis shows genome positions in base pairs. H3K9me2 data are from [1].
doi:10.1371/journal.pgen.1001334.g002

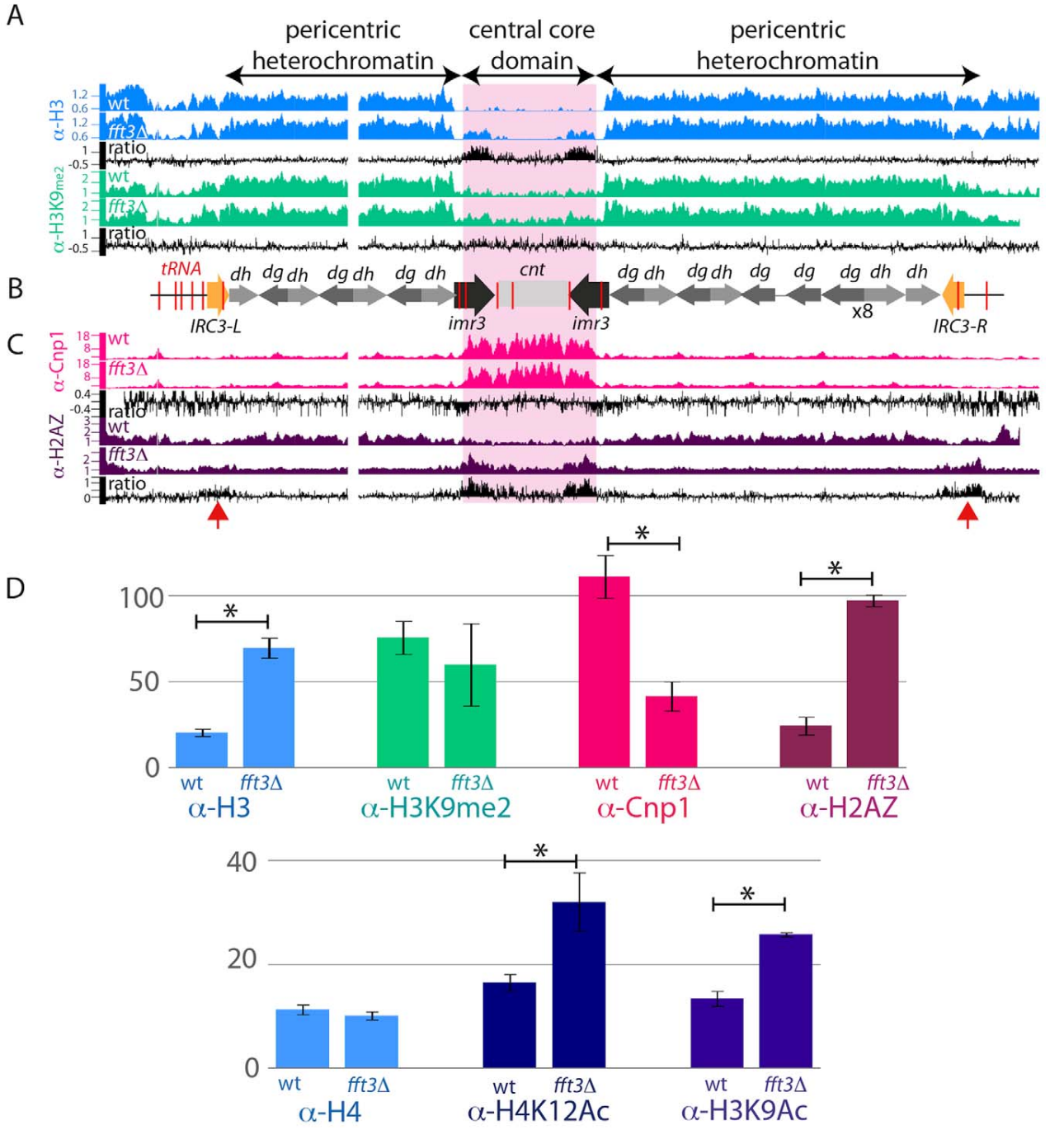

Figure 3. Centromeric boundary function is impaired in *fft3Δ* cells. A) The ChIP-chip distributions of histone H3 (blue) and H3K9me2 (green) at centromere 3 in wt and *fft3Δ* cells are shown in Genome Browser images. Y-axis: Linear scale. Mutant/wt ratios are indicated in black in log2 scale. B) A schematic diagram of centromere 3. tRNA genes are marked in red and the *IRC* elements in yellow. C) Genome browser images showing ChIP-chip data for Cnp1 (red) and H2A.Z^{Pht1} (purple). Y-axis: Linear scale. Mutant/wt ratios are shown in black in log2 scale. D) Bar diagrams showing the results from real-time quantitative PCR analysis of ChIP signals. The enrichments at *imr3* are relative to the *act1+* euchromatic control locus except for the Cnp1 enrichment which is relative to *cen1*. The ChIP signals were normalized to input samples from the same chromatin extract. The error bars represent S.D. values from triplicate samples. *indicates a significant difference between wt and mutant ($P<0.01$; T-test, two-tailed, unpaired).
doi:10.1371/journal.pgen.1001334.g003

cells (Figure 3C (red), and 3D). Outside the *imr* and central core domain the Cnp1 signals are very low (near background) in wild type and sometimes even lower in *fft3Δ* cells. Therefore, since the Cnp1 protein is basically undetectable in these regions we do not think the ratio changes observed outside the *imr* and central core regions are biologically meaningful.

Several insulators have been shown to stop the propagation of heterochromatin [11,13,16]. Therefore, we wanted to investigate

whether the H3 that appears in the central core region in *fft3Δ* cells is methylated at lysine 9. Our ChIP-chip and ChIP/quantitative PCR experiments revealed that the H3 was not methylated at K9 (Figure 3A (green) and 3D). Surprisingly, we found that the H3 that appears in the *imr* region in *fft3Δ* instead was acetylated at K9. We observed a 2-fold increase of H3K9ac in *fft3Δ* compared to wt (P value, 0.006; T-test; Figure 3D). We also found that the degree of acetylation of histone H4 at K12 was 2-fold increased at *imr3* in *fft3Δ* (P value 0.01; T-test; Figure 3D, bottom panel), but the histone H4 levels remained unchanged. Both of these acetylation marks, and especially H3K9ac, are characteristic of active euchromatin in *S. pombe* [27].

Histone H2A.Z is a universally conserved histone variant that replaces the conventional H2A protein in a significant fraction of nucleosomes [3]. Normally H2A.Z is absent from all centromeric regions, including both the Cnp1 containing inner domain and the pericentric heterochromatin [3]. Surprisingly, we observed that in the absence of Fft3, the H2A.Z levels increase by 4-fold at *imr3* (P value 0.00003; T-test; Figure 3C (purple), and 3D). Moreover, in *fft3Δ* cells, the H2A.Z levels clearly increased at *ICR* elements and at the tRNA genes flanking the pericentric regions (see red arrows in Figure 3). In euchromatin H2A.Z is localized to gene promoters and correlates well with H3K9ac and H4K12ac [3]. Taken together these results indicate that Fft3 has a novel role at insulator elements shielding the centromeric central core domain from euchromatin formation.

The above experiments show that the properties of the central core domains are altered in the *fft3Δ* mutant. Next, we wanted to investigate whether the pericentric heterochromatin domains are also affected. Paradoxically, heterochromatin domains in *S. pombe* are more sensitive to cleavage of the micrococcal nuclease (MNase) indicating a reduced nucleosome density [28,29]. The heterochromatin showed a reduced sensitivity to MNase in the *fft3Δ* mutant cells, indicating an altered chromatin structure (Figure 4 and Figure S4). Thus, Fft3 is required for a proper chromatin structure of both the pericentric and the central core chromatin domains.

Fft3 represses subtelomeric genes

Our experiments indicated that Fft3 is required to maintain a proper centromeric chromatin structure. Although Fft3 is localized to centromeres, it is possible that Fft3 also affects centromeres via changes in gene expression of centromeric components. To address this concern, expression profiling of *fft3Δ* cells was performed. mRNA from logarithmically growing *fft3Δ* cells was compared to mRNA from wild type cells. Using a 2-fold cutoff for changes in gene expression, we found that 61 genes were up-regulated and 15 genes were down-regulated in *fft3Δ* versus wild type. Importantly, no genes known to be involved in centromere function are affected, thus arguing against any indirect effects of Fft3 on centromeric chromatin.

Interestingly, further analysis of the expression profiling data revealed that, more than half of the up-regulated genes (61%) lay within the subtelomeric regions of chromosomes 1 and 2 (Figure 5). Moreover, 74% of the upregulated genes on chromosome 2 are located within 100 kb from the chromosome ends (Figure 5B). This clustering of affected genes near *tel2* is highly significant (5.39e-44, hypergeometric probability). Thus, in addition to its role in protecting centromeric chromatin domains, Fft3 is also ensuring a proper silent chromatin structure at the subtelomeres.

Fft3 counteracts euchromatin formation in subtelomeric regions

Fft3 could perform its telomeric gene silencing function directly or indirectly: (1) Fft3 could be located all over the telomeric silenced domain and facilitate subtelomeric chromatin-assembly; (2) It could function at the silenced genes themselves by binding and repressing their promoters; or (3) it may function as a component of an insulator that maintains the integrity of the subtelomeric domains. To distinguish between these possibilities, we analyzed the Fft3-myc ChIP-chip data. We found that the most prominent noncentromeric peaks of Fft3 were seen about 100 kb away from the telomeres (red arrows in Figure 6A), strongly suggesting that Fft3 has a function at subtelomeric boundaries.

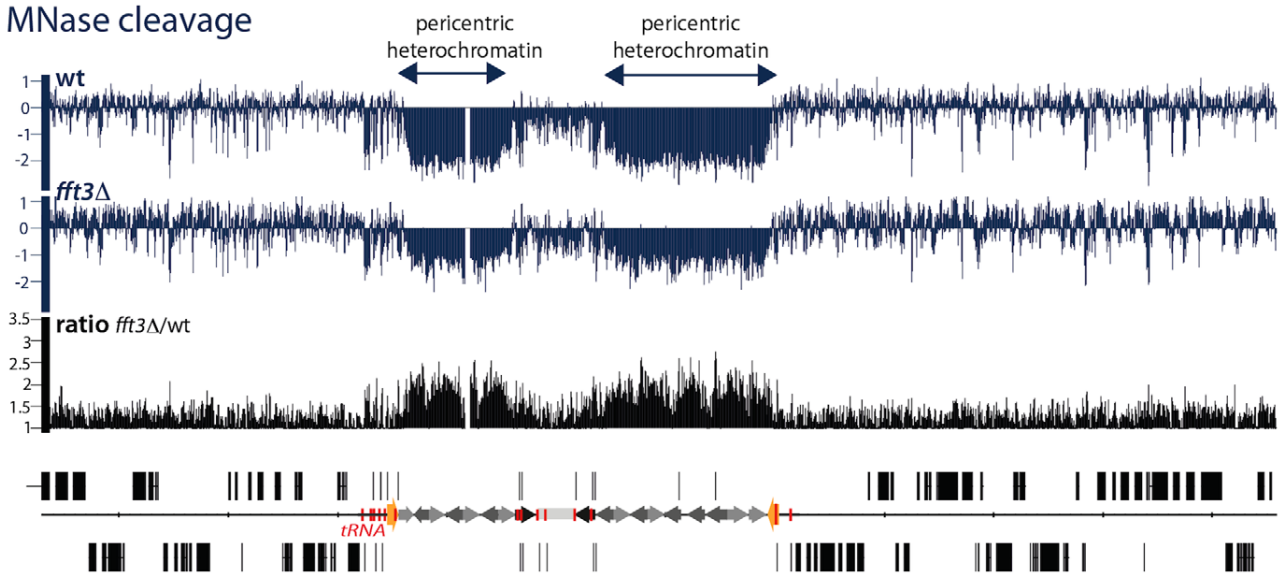

Figure 4. Fft3 is affecting chromatin structure at pericentric heterochromatin. A genome browser view showing MNase cleavage maps (blue) from wt and *fft3Δ* cells. Y-axis: Log2 scale. Data are from [28]. The mutant/wt ratio is shown in black in linear scale. tRNA genes are shown in red and IRC elements in yellow.
doi:10.1371/journal.pgen.1001334.g004

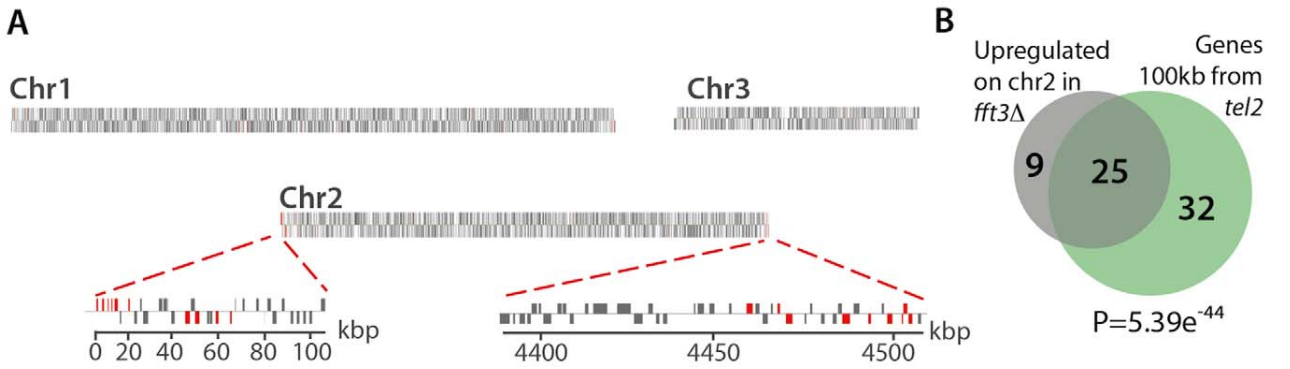

Figure 5. Fft3 is required for silencing of subtelomeric genes. A) Chromosomal view of gene expression changes in *fft3Δ* versus wt. The position of upregulated genes (2-fold cutoff) is indicated in red. The subtelomeric regions of chromosome 2 are shown in more detail. B) Venn diagram showing the overlap between genes upregulated on chromosome 2 in *fft3Δ* cells and all subtelomeric genes 100 kb from *tel2*. The P value represents the hypergeometric probability.
doi:10.1371/journal.pgen.1001334.g005

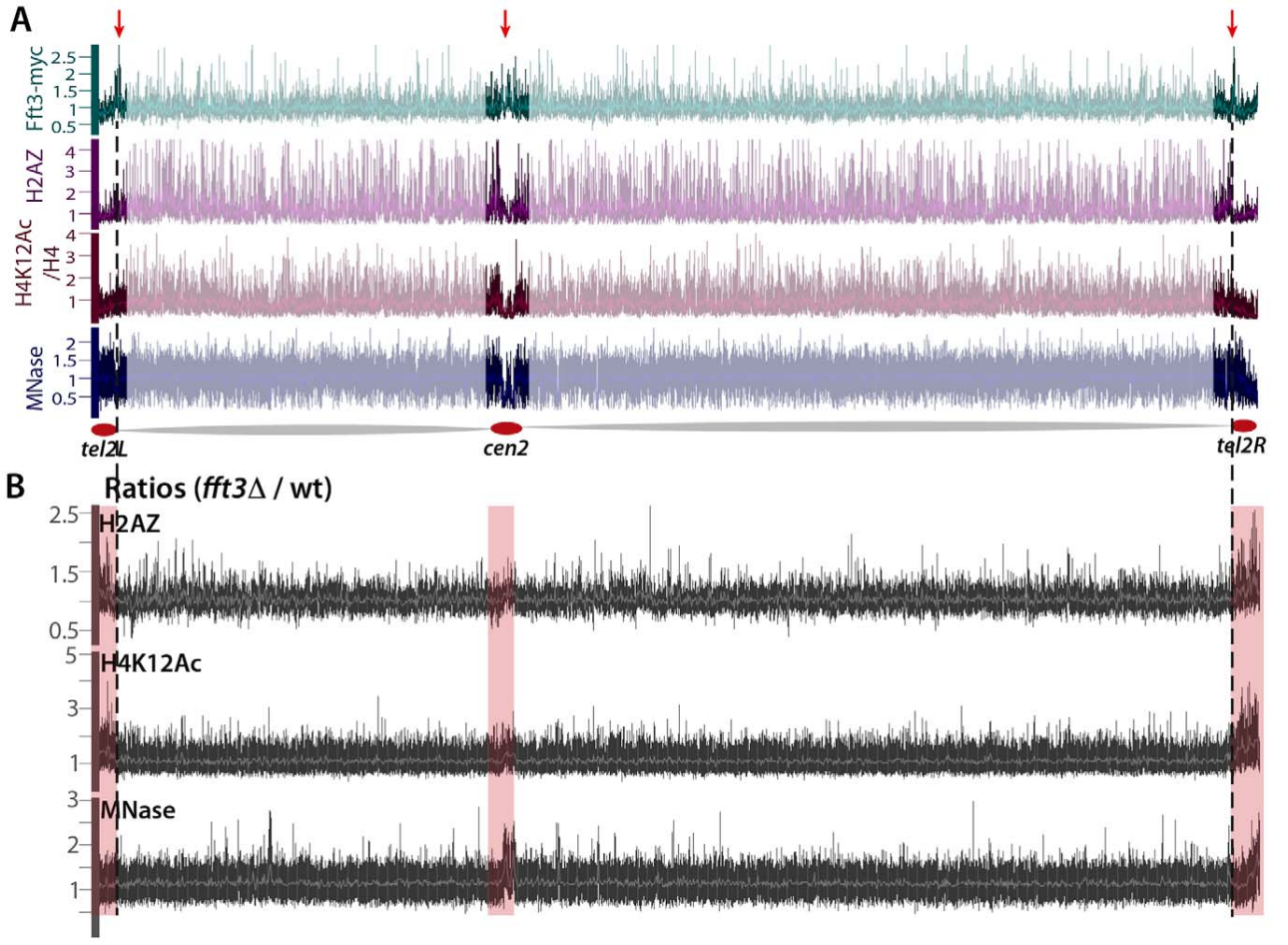

Figure 6. Fft3 is localized at subtelomeric boundaries and prevents euchromatin assembly in ST-chromatin. A) Genome browser images showing the chromosome 2 occupancy of Fft3-myc (green, Y-axis: Log2 scale), H2A.Z in wt (purple, Y-axis: linear scale), H4K12ac in wt corrected for H4 occupancy (dark red, Y-axis: linear scale), and Micrococcal Nuclease (MNase) digested chromatin in wt (blue, Y-axis: linear scale). The MNase data are from [28]. B) Genome browser views showing mutant/wt ratios for H2A.Z and H4K12ac ChIP-chip, and for MNase digested chromatin. Centromeric and subtelomeric regions are highlighted with light-pink rectangles.
doi:10.1371/journal.pgen.1001334.g006

We recently showed that the subtelomeric regions represent a distinct class of chromatin, subtelomeric chromatin (ST-chromatin), with different properties than bulk eu- or heterochromatin [3]. ST-chromatin is characterized by depletion of acetylated histones (including histone H4K12 acetylation), H3K4 methylation and H2A.Z. At the very end of the chromosome arms, there is a transition from ST-chromatin to bulk subtelomeric heterochromatin methylated on H3K9 (Figure S5).

The transition between euchromatin and the ST-chromatin is sharp, with a drastic reduction of H2A.Z, H4K12ac and H3K4me (Figure 6A and [3]). Interestingly, the peaks of Fft3 occupancy appear to be situated exactly over these transitions (see the red arrows in Figure 6A), suggesting the Fft3 binding could mark the transition from euchromatin to ST-chromatin. To explore this further, we performed ChIP-chip experiments for H2A.Z and H4K12ac in wild type and *fft3Δ* mutant cells. Our analysis shows that, when Fft3 is removed, these two euchromatin marks expand beyond the euchromatin domain into the ST-chromatin (see ratios in Figure 6B, and Figure S6). These results strongly indicate that Fft3 protects both centromeric chromatin and ST chromatin from euchromatin assembly.

Paradoxically, in *S. pombe*, heterochromatin has a wider spacing between nucleosomes and a lower nucleosome occupancy as compared to euchromatin [28,29]. To address whether Fft3 is affects the chromatin structure of heterochromatin domains, we compared the MNase digestion patterns of wild type and *fft3Δ* cells. Deletion of Fft3 did not detectably alter the global chromatin structure (Figure 6B, Figure S7, and [28]). However, our data revealed striking changes in the MNase digestion patterns across the centromeric and ST-chromatin. There is a tendency for a reduced MNase digestion in *fft3Δ* as compared to wild type cells, indicating that pericentric heterochromatin domains and ST-chromatin become more euchromatic.

From these data we conclude that Fft3 marks the boundaries between euchromatin and subtelomeres and that it prevents euchromatin formation in the ST-chromatin domains.

Altered chromatin structure at the *tel2L* subtelomeric transition zone

As described above, Fft3 is localized at the transition zone between euchromatin and ST-chromatin. At the left subtelomere on chromosome II, this transition zone coincides exactly with the presence of four long terminal repeats (LTRs) located just upstream of the promoters of four copies of one gene encoding a membrane transporter (Figure 7A). The four LTR elements, the four transporter genes, and the sequences between them are 100% identical at the nucleotide level, suggesting that this region arose from gene duplication events. At this transition a sharp decrease in

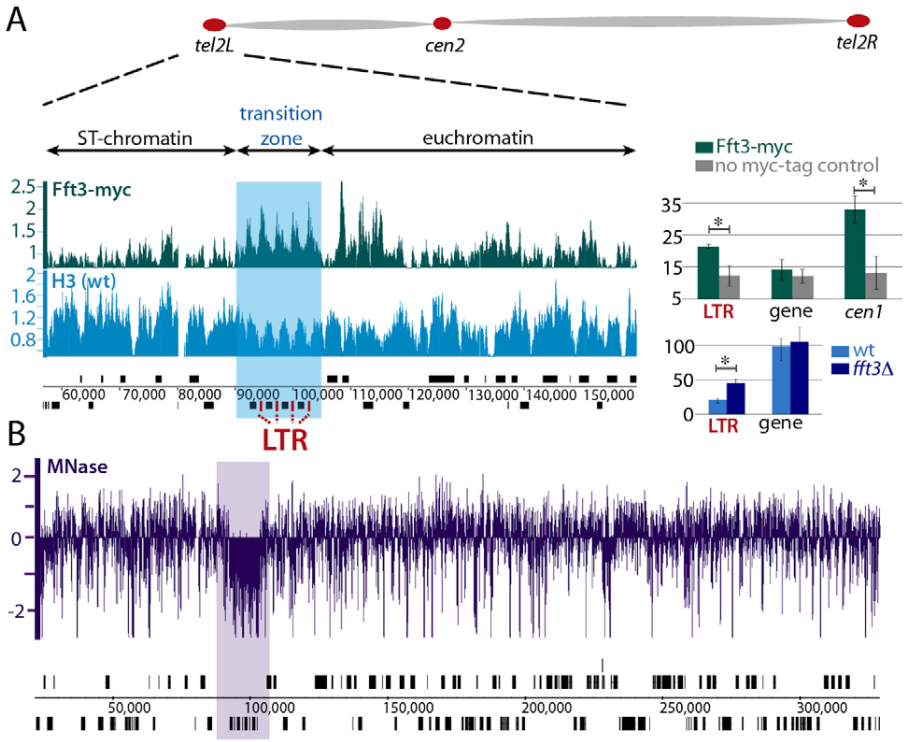

Figure 7. Fft3 is localized to the *tel2L* subtelomeric transition zone. A) Left panel: A genome browser view of subtelomere *2L*. ChIP-chip data for Fft3-myc (green) and H3 (blue) are shown. A subtelomeric transition zone consisting of four copies of a membrane transporter gene and four LTR elements (red) is highlighted in blue. Right panel (top): Bar diagrams showing quantification of Fft3-myc ChIP signals by real time PCR. Enrichment at LTR elements, membrane transporter genes (using primers for SPBPB10D8.05c), and *cnt1* was measured relative to centromeric *dg* repeats. Background normalization was performed using -antibody samples. The grey bars represent signals from the non-tagged control strain (Hu29). The error bars represent S.D. values from triplicate samples. *indicates a significant difference between Fft3-myc and the non-tagged control strain ($P<0.01$; T-test, two-tailed, unpaired). Right panel (bottom): Bar diagrams showing quantification of H3 ChIP in wt (blue) and *fft3Δ* (black) on LTR elements and membrane transporter genes relative to an euchromatin control gene (SPAC32A11.03c). The ChIP signals were normalized to input samples from the same chromatin extract. The error bars represent S.D. from triplicate samples. *indicates a significant difference between wt and *fft3Δ* cells ($P<0.01$; T-test, two-tailed, unpaired). B) A genome browser view of mononucleosomal signals in wt after MNase digestion. Data are from [28].

doi:10.1371/journal.pgen.1001334.g007

H2A.Z, H4K12ac and H3K4me2 is seen (Figure 6 and Figure S5), indicating that this region might function as an insulator element.

Insulators and barrier elements are often characterized by a special chromatin structure that manifests itself as a constitutive DNaseI hypersensitive site [30–32]. It has been suggested that hypersensitive sites signify a disruption of the regular nucleosome repeat along the DNA fiber and that they function as binding sites for sequence-specific factors. In agreement with this notion, we found that the LTR region was highly sensitive to MNase cutting (Figure 7B), indicating that this region has typical features of an insulator.

Analysis of the Fft3 occupancy map revealed that Fft3 is present at these LTR sequences, but not at the membrane transporter genes (Figure 7A). The ChIP-chip data also revealed that histone H3 is enriched over the transporter genes coding regions and depleted from the intergenic regions and the LTR elements. The occupancy of Fft3 at LTR elements was confirmed by quantitative PCR analysis. Interestingly, quantitative PCR also showed that the H3 density at the LTRs was increased about 2-fold in *fft3Δ* cells ($P = 0.002$; T-test), while the H3 density at the membrane transporter genes remained unchanged. This suggests that Fft3 is interacting with the LTR sequences where it stimulates nucleosome disassembly or eviction. Thus, Fft3 is required for a proper chromatin structure of a subtelomeric transition zone.

Discussion

Active and silent chromatin domains are often juxtaposed along the chromosome arms, but they need to be separated in order to maintain chromosome stability and correct gene expression levels. The spreading of chromatin domains beyond their natural borders is blocked by insulators. Previous studies have identified such elements surrounding the heterochromatin domains in fission yeast, but the mechanisms of boundary function are not well understood.

In *S. pombe*, all described insulators act as barrier elements that restrict the spread of silenced chromatin [11,13,16]. In this study we describe a mechanism in which euchromatin is blocked from entering certain chromatin domains. Our study shows that Fft3, an ATP-dependent chromatin-remodeling factor, is localized to known centromeric insulators and at a subtelomeric transition zone. In cells depleted for Fft3, euchromatin is assembled in the centromeric central cores and subtelomeric chromatin domains, involving a change of histone modifications, incorrect incorporation of histone variants and mis-regulation of gene expression. This strongly suggests that Fft3 controls the identity of chromatin domains by shielding them from euchromatin formation.

S. pombe utilizes at least two independent pathways to maintain silent heterochromatin at telomeres [33]. The first pathway involves Taz1, a homolog of mammalian TRF1/2, which binds directly to the telomere-associated sequence (TAS) and recruits factors essential for heterochromatin formation [34]. The other pathway requires another *cis* acting element consisting of *cenH*-like sequences that display extensive sequence homology with the *dg* and *dh* repeats found at centromeres. These repeats function as DNA templates for siRNA production. The siRNA are processed by the RNAi-RITS pathway [1,33] and histones become methylated on histone H3 at lysine 9. H3K9me then spreads inward along the chromosome arms. Approximately 20 kb into the chromosome arms, the spreading of H3K9me terminates and instead ST-chromatin is formed [3]. The mechanism of this transition is not understood. A second transition occurs around 100 kb, where ST-chromatin is replaced by bulk euchromatin. This transition is relatively sharp with large changes of H2A.Z and H4K12ac levels. In this study, we have shown that Fft3 plays an important role in this second transition. When Fft3 is removed, the integrity of ST-chromatin is lost. Euchromatin marks, such as histone acetylation and enrichment of histone variant H2AZ appear instead. As a result of this, genes in the normally silent subtelomere become expressed. In agreement with this, we showed from MNase cleavage patterns that the telomeric chromatin structure is changed and becomes more euchromatin-like in *fft3Δ* mutant cells. Interestingly, two independent studies found that Fft3 co-purifies with the heterochromatic Swi6 protein[35] [36]. It is possible that this interaction is important to protect the integrity of the subtelomere chromatin structure.

Fft3 is localized to a subtelomeric transition zone containing genes and LTR elements arisen from gene duplication events. Duplicated segments at transition zones seem to be a conserved feature. In human, more than half of the transition regions between euchromatin and centromeric heterochromatin contain duplicated segments and multiple duplicones are concatenated together to form larger block of wall-to-wall duplications [37]. Interestingly, it has been demonstrated that two demethylases, Lsd1 and Lsd2, with roles in centromeric boundary function, are also localized to the *S. pombe tel2L* transition zone. The demethylases are present at the promoters of the membrane transporter genes where they demethylate H3K9me3 [16].

We could also show that Fft3 regulates the chromatin structure at the centromeres. In *fft3Δ* mutant cells H3 levels are increased and Cnp1 levels are reduced in the central core domain. Previously described centromeric insulators inhibit heterochromatin spreading [11,13,16]. Fft3 is located at these elements but does not participate in the heterochromatin blocking. Instead, similarly to what happens at subtelomeres, we see euchromatin marks such as histone acetylation and H2A.Z appearing in the central core region in the absence of Fft3. We propose that the insulator elements at centromeres have a novel function in addition to heterochromatin barrier function. This additional function involves Fft3 mediated protection from euchromatin formation in the central core region. It is not clear what the 'source' of the newly formed euchromatin is which renders the centromere dysfunctional and leads to severe chromosome segregation defects. Simple spreading models can be ruled out since the central core region is flanked by pericentric heterochromatin. The euchromatin assembly could be mediated by recruitment of trans-acting components. Alternatively it could spread from the euchromatin regions that are flanking the pericentric heterochromatin. In this scenario the pericentric regions would be skipped by looping out of the pericentric domain via clustering of the tRNAs in *imr* and *IRC* regions.

Insulator elements that protect chromosome domains from euchromatin have previously been described in *Drosophila*. For example, the *scs* and *scs'* (specialized chromatin structures) elements insulate the expression of the *white* reporter gene from euchromatin [38], and boundaries between bithorax domains protect inactive domains from the open configuration of the neighboring domain [39]. It has been suggested that insulator elements exert their function by partitioning chromosomal domains into "higher-order" loops either by interacting with each other or with fixed nuclear structure such as the nuclear matrix or nuclear pores [10,11,40,41]. It has been suggested that *S. pombe* also uses a looping mechanism to create functional insulator elements. The Pol III transcription factor TFIIIC is recruited to insulator elements flanking the mating loci and is thought to tether these boundaries to the nuclear periphery [11]. In addition, tRNA and other Pol III transcribed genes dispersed throughout the chromosomes localize to the nuclear periphery at centromeres,

and this localization is mediated by condensin [42]. Fft3 is localized to tRNA genes both in fission and budding yeast [43] and it is possible that Fft3 somehow cooperates with condensin in the tethering of tRNA to the centromere.

The *Drosophila* Su(Hw) (suppressor of hairy-wing) insulator protein form insulator bodies that interact with the nuclear matrix. This tethering to the matrix is required for its insulating function [7]. Moreover, the vertebrate insulator protein CTCF also interacts with the nuclear matrix [44]. Interestingly, it was recently shown that Fft3 also is tightly associated with the nuclear matrix [45].

A synthetic screen for barrier activity in *S. cerevisiae* identified proteins involved in nuclear transport as insulator proteins [10]. Since transport proteins localize to the nuclear pore complex, these results led to the model that tethering insulators to nuclear pores aids in the formation of loops. Recently, it was shown that Fft3 binds to the Ran nuclear transporter Spi1 [45] and *fft3Δ* shows synthetic lethality with mutations of several genes encoding nuclear transport proteins and nucleoporins [46]. This indicates that Fft3 maybe involved in forming chromatin loops by attaching insulator elements to the nuclear matrix or pores. This would isolate a signal generated in one chromatin domain from reaching the domain in the next loop. This could explain how Fft3 shields off centromeres and subtelomeres from euchromatin formation.

The Fun30 family of chromatin remodeling factors, represented by SMARCAD1 in humans [47], Etl1 in mouse [48], and Fun30 in budding yeast [18] is a group of conserved proteins that has received little attention and their molecular functions are relatively unknown. We have shown that the *S. pombe* FUN30 homolog, Fft3, protects centromeres and subtelomeres from euchromatin. This type of insulating activity could to be a conserved property of the FUN30 chromatin remodeling factors. It was recently shown that the *S. cerevisiae* homolog, FUN30, binds and alters the nucleosome positioning at the *HMR* barrier element and is required for silencing of the *HMR* domain [43]. Thus it is possible that FUN30 in budding yeast has a similar shielding function as Fft3 in fission yeast. Our study identifies a new biological function for the Fun30 class of chromatin remodeling factors at centromeres and in ST-chromatin, and expands our understanding of the molecular composition and machinery involved in partitioning neighboring chromatin domains. Further characterization of insulators and their role in preserving distinct chromatin configurations will help us better understand the higher order organization of chromosomes.

Materials and Methods

S. pombe strains used are listed in Table S1. Standard procedures were used for growth and genetic manipulation.

Central core silencing assay

Cell suspensions of wild type (FY412) and *fft3Δ* (Hu1321) strains were 5-fold diluted, spotted on non-selective plates (PMG), - ura plates, and counter-selective FOA plates (1.0 g/l, US Biologicals) and incubated at 30°C for 3 days.

Ura4 expression profiling

Total RNA was extracted from Hu303 (wild-type), FY412 (*CC2::ura4+*), Hu1321 (*fft3Δ CC2::ura4+*), FY340 (*TM1::ura* random integrant), and Hu111 (*ura4-DS/E*) as described earlier [49]. Contaminating DNA was removed with TURBO DNA-free kit (ambion). RT-PCR was performed using SuperScipt II Reverse Transcriptase (invitrogen) and Oligo$(dT)_{12-18}$ primers (invitrogen). The primers used for the *ura4* PCR are listed in Table S2.

ChIP-chip

DNA was immunoprecipitated as described earlier [50], using 10 µl of anti-Cnp1 antiserum, 2 µl of anti-myc (9E10), 2 µl of anti-H4K12ac (ab1761, abcam), 1.5 µg of anti H3 (ab1791, abcam), 2 µl of anti-H4 (Pan 05-858, upstate), 5 µg of anti-H3K9me2 (07-441, upstate), or 2 µl of anti-H3K9Ac (07-352, Millipore) antibodies per 100 µl chromatin extract.

Real-time quantitative PCR was preformed in the presence of SYBR Green using the Applied Biosystems 7500 real-time PCR machine. The primers used are listed in Table S2.

H3K9me Chip-chip data (Figure 2, Figure S2, and Figure S5) and genome-wide MNase digestion maps are from previous studies [1,28].

Microarray analysis

Immunoprecipitated DNA was amplified to 5 µg DNA as described in [50], with the exception that in the second PCR 5 mM dUTP was added to the reaction.

Fragmentation, labeling and hybridization to the Affymetrix GeneChip S. *pombe* Tiling 1.0FR was performed by Affymetrix core facility at Novum (BEA) according to Affymetrix standard protocols.

Raw data from Affymetrix (.CEL format) were analyzed with Affymetrix Tiling Analysis Software (TAS) v1.1 and visualized with Affymetrix Integrated Genome Browser (IGB). A tiling analysis group (.TAG file) for a two-sample analysis containing 2 ChIP experiments as the 'treatment' group and 2 input samples as the 'control' group was created in TAS. The data were normalized using quantile normalization plus scaling and run with a bandwidth of 20.

Microarray data have been deposited in the ArrayExpress database (http://www.ebi.ac.uk/arrayexpress/) under the accession code E-MEXP-3044.

Expression profiling

Total RNA from wild type and *fft3Δ* strains was purified as described earlier [49] and hybridized to Affymetrix GeneChip S. *pombe* Tiling 1.0FR according to protocol and recommendations from Affymetrix. Data was normalized in TAS as described above and normalized data was analyzed using GeneSpring software (Agilent). A standard cutoff value of 2-fold was used for gene expression changes.

Supporting Information

Figure S1 A) Top: A schematic map of *S. pombe* centromere 2. The central core domain (*cnt* and *imr*) is surrounded by outer repeat regions (*dh* and *dg*). *Ura4+*insertion at *cnt2* allows the monitoring of silencing at the central core. Bottom: Silencing of *cen2: ura4+* in Hu303 (wt), FY412 (*CC2::ura4*) and Hu1321 (*fft3Δ CC2::ura4*). Growth was assayed on non-selective (N/S), uracil depleted (-URA), or counter-selective (FOA) plates. B) RT-PCR of *ura4* expression. URA4− DS/E indicates bands amplified from the authentic gene with a 280 bp deletion. * show a shadow band.
Found at: doi:10.1371/journal.pgen.1001334.s001 (2.93 MB TIF)

Figure S2 A) A genome browser view of *cen1* showing the Chip-chip binding profile for Fft3-myc (green), H3K9me2 (black) and Cnp1 (pink) (log2 scale). H3K9me2 data are from Cam et al. 2005 [1]. B) A genome browser view of *cen2*.
Found at: doi:10.1371/journal.pgen.1001334.s002 (3.69 MB TIF)

Figure S3 A) The ChIP-chip distributions of histone H3 (blue) and H3K9me2 (green), Cnp1 (red), and H2A.Z (purple) at

centromere 1 in wt and *fft3Δ* cells are shown in Genome Browser images. Mutant/wt ratios are indicated in black. Linear scale. B) Genome browser view of centromere II.
Found at: doi:10.1371/journal.pgen.1001334.s003 (5.80 MB TIF)

Figure S4 A) A genome browser view showing MNase cleavage maps of centromere I from wt and *fft3Δ* cells. Log2 scale. The ratio is shown in black. tRNA genes are shown in red and IRC elements in yellow. Data are from Lantermann et al, 2010 [28]. B) Same as above for centromere II.
Found at: doi:10.1371/journal.pgen.1001334.s004 (3.77 MB TIF)

Figure S5 A genome browser view showing left arm of chromosome II. Chip-chip for H3K9me2, H3K4me2, and Fft3-myc (green) are shown. Log2 scale. H3K9me2 and H3K4me2 data are from Cam et al. 2005 [1].
Found at: doi:10.1371/journal.pgen.1001334.s005 (1.93 MB TIF)

Figure S6 A) A genome browser view of chromosome I, showing the genome-wide ChIP-chip density of H2A.Z^{Pht1} (purple) and H4K12ac corrected for H4 occupancy (red). The ratios (*fft3Δ*/wt) are shown in dark grey. Linear scale. B) A genome browser view of chromosome III.
Found at: doi:10.1371/journal.pgen.1001334.s006 (7.43 MB TIF)

Figure S7 A) Chromatin from wt and *fft3Δ* cells was digested with micrococcal nuclease (MNase) and hybridized to microarrays. Chromosome I is shown in a genome browser view. The ratio (*fft3Δ*/wt) is shown in dark grey. Data are from Lantermann et al. 2010 [28]. B) As above for chromosome III.
Found at: doi:10.1371/journal.pgen.1001334.s007 (4.42 MB TIF)

Table S1 List of strains used in this study.
Found at: doi:10.1371/journal.pgen.1001334.s008 (0.06 MB DOC)

Table S2 List of primers used in this study.
Found at: doi:10.1371/journal.pgen.1001334.s009 (0.03 MB DOC)

Acknowledgments

We thank Jenna Persson for critical reading of the manuscript. We would also like to thank the Affymetrix core facility at Novum, BEA, for the help with microarray analysis.

Author Contributions

Conceived and designed the experiments: AS JW HB KE. Performed the experiments: AS JW HB. Analyzed the data: AS. Contributed reagents/materials/analysis tools: AS KE. Wrote the paper: AS KE.

References

1. Cam HP, Sugiyama T, Chen ES, Chen X, FitzGerald PC, et al. (2005) Comprehensive analysis of heterochromatin- and RNAi-mediated epigenetic control of the fission yeast genome. Nat Genet 37: 809–819.
2. Noma K, Allis CD, Grewal SI (2001) Transitions in distinct histone H3 methylation patterns at the heterochromatin domain boundaries. Science 293: 1150–1155.
3. Buchanan L, Durand-Dubief M, Roguev A, Sakalar C, Wilhelm B, et al. (2009) The Schizosaccharomyces pombe JmjC-protein, Msc1, prevents H2A.Z localization in centromeric and subtelomeric chromatin domains. PLoS Genet 5: e1000726. doi:10.1371/journal.pgen.1000726.
4. Hebbes TR, Clayton AL, Thorne AW, Crane-Robinson C (1994) Core histone hyperacetylation co-maps with generalized DNase I sensitivity in the chicken beta-globin chromosomal domain. EMBO J 13: 1823–1830.
5. Braunstein M, Rose AB, Holmes SG, Allis CD, Broach JR (1993) Transcriptional silencing in yeast is associated with reduced nucleosome acetylation. Genes Dev 7: 592–604.
6. Noma K, Sugiyama T, Cam H, Verdel A, Zofall M, et al. (2004) RITS acts in cis to promote RNA interference-mediated transcriptional and post-transcriptional silencing. Nat Genet 36: 1174–1180.
7. Dorman ER, Bushey AM, Corces VG (2007) The role of insulator elements in large-scale chromatin structure in interphase. Semin Cell Dev Biol 18: 682–690.
8. Oki M, Valenzuela L, Chiba T, Ito T, Kamakaka RT (2004) Barrier proteins remodel and modify chromatin to restrict silenced domains. Mol Cell Biol 24: 1956–1967.
9. Dhillon N, Raab J, Guzzo J, Szyjka SJ, Gangadharan S, et al. (2009) DNA polymerase epsilon, acetylases and remodellers cooperate to form a specialized chromatin structure at a tRNA insulator. EMBO J 28: 2583–2600.
10. Ishii K, Arib G, Lin C, Van Houwe G, Laemmli UK (2002) Chromatin boundaries in budding yeast: the nuclear pore connection. Cell 109: 551–562.
11. Noma K, Cam HP, Maraia RJ, Grewal SI (2006) A role for TFIIIC transcription factor complex in genome organization. Cell 125: 859–872.
12. Wood V, Gwilliam R, Rajandream MA, Lyne M, Lyne R, et al. (2002) The genome sequence of Schizosaccharomyces pombe. Nature 415: 871–880.
13. Scott KC, Merrett SL, Willard HF (2006) A heterochromatin barrier partitions the fission yeast centromere into discrete chromatin domains. Curr Biol 16: 119–129.
14. Scott KC, White CV, Willard HF (2007) An RNA polymerase III-dependent heterochromatin barrier at fission yeast centromere 1. PLoS ONE 2: e1099. doi:10.1371/journal.pone.0001099.
15. Oki M, Kamakaka RT (2005) Barrier function at HMR. Mol Cell 19: 707–716.
16. Lan F, Zaratiegui M, Villen J, Vaughn MW, Verdel A, et al. (2007) S. pombe LSD1 homologs regulate heterochromatin propagation and euchromatic gene transcription. Mol Cell 26: 89–101.
17. Thon G, Bjerling P, Bunner CM, Verhein-Hansen J (2002) Expression-state boundaries in the mating-type region of fission yeast. Genetics 161: 611–622.
18. Ouspenski II, Elledge SJ, Brinkley BR (1999) New yeast genes important for chromosome integrity and segregation identified by dosage effects on genome stability. Nucleic Acids Res 27: 3001–3008.
19. Takahashi K, Chen ES, Yanagida M (2000) Requirement of Mis6 centromere connector for localizing a CENP-A-like protein in fission yeast. Science 288: 2215–2219.
20. Takahashi K, Yamada H, Yanagida M (1994) Fission yeast minichromosome loss mutants mis cause lethal aneuploidy and replication abnormality. Mol Biol Cell 5: 1145–1158.
21. Clarke L, Amstutz H, Fishel B, Carbon J (1986) Analysis of centromeric DNA in the fission yeast Schizosaccharomyces pombe. Proc Natl Acad Sci U S A 83: 8253–8257.
22. Chikashige Y, Kinoshita N, Nakaseko Y, Matsumoto T, Murakami S, et al. (1989) Composite motifs and repeat symmetry in S. pombe centromeres: direct analysis by integration of NotI restriction sites. Cell 57: 739–751.
23. Nakayama J, Rice JC, Strahl BD, Allis CD, Grewal SI (2001) Role of histone H3 lysine 9 methylation in epigenetic control of heterochromatin assembly. Science 292: 110–113.
24. Partridge JF, Borgstrom B, Allshire RC (2000) Distinct protein interaction domains and protein spreading in a complex centromere. Genes Dev 14: 783–791.
25. Allshire RC, Javerzat JP, Redhead NJ, Cranston G (1994) Position effect variegation at fission yeast centromeres. Cell 76: 157–169.
26. Bi X, Yu Q, Sandmeier JJ, Zou Y (2004) Formation of boundaries of transcriptionally silent chromatin by nucleosome-excluding structures. Mol Cell Biol 24: 2118–2131.
27. Wiren M, Silverstein RA, Sinha I, Walfridsson J, Lee HM, et al. (2005) Genomewide analysis of nucleosome density histone acetylation and HDAC function in fission yeast. EMBO J 24: 2906–2918.
28. Lantermann AB, Straub T, Stralfors A, Yuan GC, Ekwall K, et al. (2010) Schizosaccharomyces pombe genome-wide nucleosome mapping reveals positioning mechanisms distinct from those of Saccharomyces cerevisiae. Nat Struct Mol Biol 17: 251–257.
29. Garcia JF, Dumesic PA, Hartley PD, El-Samad H, Madhani HD (2010) Combinatorial, site-specific requirement for heterochromatic silencing factors in the elimination of nucleosome-free regions. Genes Dev 24: 1758–1771.
30. Udvardy A, Maine E, Schedl P (1985) The 87A7 chromomere. Identification of novel chromatin structures flanking the heat shock locus that may define the boundaries of higher order domains. J Mol Biol 185: 341–358.
31. Chung JH, Whiteley M, Felsenfeld G (1993) A 5′ element of the chicken beta-globin domain serves as an insulator in human erythroid cells and protects against position effect in Drosophila. Cell 74: 505–514.
32. Nasmyth KA (1982) The regulation of yeast mating-type chromatin structure by SIR: an action at a distance affecting both transcription and transposition. Cell 30: 567–578.
33. Kanoh J, Sadaie M, Urano T, Ishikawa F (2005) Telomere binding protein Taz1 establishes Swi6 heterochromatin independently of RNAi at telomeres. Curr Biol 15: 1808–1819.
34. Cooper JP, Nimmo ER, Allshire RC, Cech TR (1997) Regulation of telomere length and function by a Myb-domain protein in fission yeast. Nature 385: 744–747.
35. Fischer T, Cui B, Dhakshnamoorthy J, Zhou M, Rubin C, et al. (2009) Diverse roles of HP1 proteins in heterochromatin assembly and functions in fission yeast. Proc Natl Acad Sci U S A 106: 8998–9003.

36. Motamedi MR, Hong EJ, Li X, Gerber S, Denison C, et al. (2008) HP1 proteins form distinct complexes and mediate heterochromatic gene silencing by nonoverlapping mechanisms. Mol Cell 32: 778–790.
37. Horvath JE, Bailey JA, Locke DP, Eichler EE (2001) Lessons from the human genome: transitions between euchromatin and heterochromatin. Hum Mol Genet 10: 2215–2223.
38. Kellum R, Schedl P (1991) A position-effect assay for boundaries of higher order chromosomal domains. Cell 64: 941–950.
39. Gyurkovics H, Gausz J, Kummer J, Karch F (1990) A new homeotic mutation in the Drosophila bithorax complex removes a boundary separating two domains of regulation. EMBO J 9: 2579–2585.
40. Gerasimova TI, Byrd K, Corces VG (2000) A chromatin insulator determines the nuclear localization of DNA. Mol Cell 6: 1025–1035.
41. Yusufzai TM, Tagami H, Nakatani Y, Felsenfeld G (2004) CTCF tethers an insulator to subnuclear sites, suggesting shared insulator mechanisms across species. Mol Cell 13: 291–298.
42. Iwasaki O, Tanaka A, Tanizawa H, Grewal SI, Noma K (2010) Centromeric localization of dispersed Pol III genes in fission yeast. Mol Biol Cell 21: 254–265.
43. Neves-Costa A, Will WR, Vetter AT, Miller JR, Varga-Weisz P (2009) The SNF2-family member Fun30 promotes gene silencing in heterochromatic loci. PLoS ONE 4: e8111. doi:10.1371/journal.pone.0008111.
44. Yusufzai TM, Felsenfeld G (2004) The 5′-HS4 chicken beta-globin insulator is a CTCF-dependent nuclear matrix-associated element. Proc Natl Acad Sci U S A 101: 8620–8624.
45. Ohba T, Nishijima H, Nishitani H, Nishimoto T (2008) Schizosaccharomyces pombe Snf2SR, a novel SNF2 family protein, interacts with Ran GTPase and modulates both RanGEF and RanGAP activities. Genes Cells 13: 571–582.
46. Roguev A, Bandyopadhyay S, Zofall M, Zhang K, Fischer T, et al. (2008) Conservation and rewiring of functional modules revealed by an epistasis map in fission yeast. Science 322: 405–410.
47. Adra CN, Donato JL, Badovinac R, Syed F, Kheraj R, et al. (2000) SMARCAD1, a novel human helicase family-defining member associated with genetic instability: cloning, expression, and mapping to 4q22-q23, a band rich in breakpoints and deletion mutants involved in several human diseases. Genomics 69: 162–173.
48. Soininen R, Schoor M, Henseling U, Tepe C, Kisters-Woike B, et al. (1992) The mouse Enhancer trap locus 1 (Etl-1): a novel mammalian gene related to Drosophila and yeast transcriptional regulator genes. Mech Dev 39: 111–123.
49. Xue Y, Haas SA, Brino L, Gusnanto A, Reimers M, et al. (2004) A DNA microarray for fission yeast: minimal changes in global gene expression after temperature shift. Yeast 21: 25–39.
50. Durand-Dubief M, Ekwall K (2009) Chromatin immunoprecipitation using microarrays. Methods Mol Biol 529: 279–295.